

An Analysis of Performance Bottlenecks in MRI Pre-Processing

Mathieu Dugré*, Yohan Chatelain, Tristan Glatard

Department of Computer Science and Software Engineering, Concordia University, Montreal, QC, Canada
research@mathdugre.me

Abstract—Magnetic Resonance Image (MRI) pre-processing is a critical step for neuroimaging analysis. However, the computational cost of MRI pre-processing pipelines is a major bottleneck for large cohort studies and some clinical applications. While High-Performance Computing (HPC) and, more recently, Deep Learning have been adopted to accelerate the computations, these techniques require costly hardware and are not accessible to all researchers. Therefore, it is important to understand the performance bottlenecks of MRI pre-processing pipelines to improve their performance. Using the Intel VTune profiler, we characterized the bottlenecks of several commonly used MRI preprocessing pipelines from the ANTs, FSL, and FreeSurfer toolboxes. We found few functions contributed to most of the CPU time, and that linear interpolation was the largest contributor. Data access was also a substantial bottleneck. We identified a bug in the ITK library that impacts the performance of ANTs pipeline in single-precision and a potential issue with the OpenMP scaling in FreeSurfer recon-all. Our results provide a reference for future efforts to optimize MRI pre-processing pipelines.

I. INTRODUCTION

Pre-processing of Magnetic Resonance Imaging (MRI) data is a critical step in neuroimaging. Although established pre-processing pipelines exist, they commonly require extensive amounts of computation and produce large volumes of output and intermediate data. Such requirements create challenges when studying large neuroimaging cohorts, and they limit clinical applicability when timely data analysis is needed. Therefore, the neuroimaging community is constantly seeking for ways to improve the computational performance of MRI pre-processing pipelines. In this paper, we characterize the computational cost of several commonly adopted MRI preprocessing pipelines, providing a reference benchmark for future efforts to optimize MRI pre-processing pipelines.

MRI is a standard tool used by neuroscientists to perform clinical diagnosis and for researchers to develop a better understanding of the brain. Three main MRI modalities exist: structural MRI (sMRI), functional MRI (fMRI), and diffusion MRI (dMRI). While other modalities such as electroencephalography (EEG), computed tomography (CT), and positron emission tomography (PET) exist, we focus on MRI for its broad adoption in research and non-invasiveness.

Neuroscientists developed various toolboxes to tackle the challenging task of pre-processing MRI data. We focus on the commonly accepted fMRIPrep [1] pipeline, as it is a comprehensive pre-processing application for both sMRI and fMRI. fMRIPrep combines several pipelines to produce a

complete pre-processing pipeline. We study fMRIPrep's sub-pipelines separately, to provide a finer grained analysis of the performance bottlenecks.

To profile the pipelines, we use the Intel VTune tool [2], a multi-language profiler with low performance overhead that provides runtime information at the level of functions. We profile the pipeline in single-threaded mode and using 32 threads to account for parallel executions. We aggregate subjects' results for each pipeline to get an average performance profile.

II. MATERIALS & METHODS

A. Pipelines

fMRIPrep is a commonly used fMRI and sMRI pre-processing pipeline for neuroimaging, built on top of several well-known neuroimaging toolboxes such as Advanced Normalization Tools (ANTs) [3], FMRIB Software Library (FSL) [4], FreeSurfer [5] and Analysis of Functional NeuroImages (AFNI) [6]. Although processing steps may vary based on the type of input data, the sMRI pipeline uses ANTs BrainExtraction [7], [8] to perform intensity correction and skull-stripping of a T1 weighted image, FSL FAST [9] to segment the tissues of the extracted brain, and ANTs registrationSyN [8] to register the segmented brain. When enabled, FreeSurfer recon-all [10] is used for surface reconstruction. We benchmarked a recon-all command similar to fMRIPrep's, which (1) performs autorecon1 without skull-stripping, (2) imports an external skull-strip from ANTs brainExtraction, and (3) resumes reconstruction with autorecon2 and autorecon3. The fMRI pipeline performs motion correction with FSL MCFLIRT [11], slice timing correction with AFNI 3dtshift [6], and co-registration with FSL FLIRT [11]–[13].

We profiled the entire fMRIPrep pipeline to get a coarse view of the pipeline's performance bottleneck. To characterize the performance at a finer grain, we profiled the default sub-pipelines of fMRIPrep listed above. While we used the same sub-pipeline and order as in fMRIPrep, we used the default parameters for most of the sub-pipelines, which may vary from the default parameters of fMRIPrep. We omitted some sub-pipelines of fMRIPrep, as they were not compatible with our dataset. For example, slice-timing correction was already performed in our data.

ANTs brainExtraction and registrationSyN are available in single or double precision, leveraging the Insight Segmentation and Registration Toolkit (ITK) [14]. We profiled both versions

to understand the performance benefits of using reduced precision in the pipelines.

B. Data

To ensure that our performance profiles are inclusive of different populations, we used data with a wide range of age and equal distribution of sex. We used the OpenNeuro ds004513 v1.0.2 dataset [15]. The anatomical and functional data from 20 healthy individuals were acquired from two different cohorts. The within-subject cohort has nine participants (mean age=43 yrs, std=7 yrs; 4 females) with two sessions: eyes open and eyes closed. The replication cohort has eleven participants (mean age=27 yrs, std=5 yrs; 6 females) with only the eyes open session. Each subject has an anatomical image with a resolution of 1 mm and a dimension of $160 \times 240 \times 256$ voxels (approx. 12 MiB). The subjects have 300 functional images taken at 2 seconds interval with a resolution of 3 mm and a dimension of $64 \times 64 \times 35$ voxels (approx. 50 MiB).

C. Profiling

Profiling MRI pre-processing pipelines raises a few challenges. Neuroimaging pipelines use several programming languages including, *C*, *C++*, *Fortran*, *Matlab*, and *Python*, with several pipelines using a combination of multiple languages. Pipelines are generally complex and computationally expensive.

The Intel VTune profiler addresses these challenges by offering multi-language support, low performance overhead, and information on functions at the runtime level. However, common profiling challenges remain. Profilers require source code to be compiled with debug symbols to report interpretable information about the different functions and modules. Different input data can substantially impact the performance results because of conditional branching in the pipeline and convergence thresholds. We discuss our approach to these challenges in the next section.

First, to get human-readable information on function and module names in VTune, we re-compiled each pipeline with debug information in a Docker image. For use on HPC systems, we created Apptainer [16] images using Docker2Singularity¹. Listing 1 demonstrates the profiling of a pipeline by mounting the VTune binary to the Apptainer image during execution.

```

1 #!/bin/sh
2 singularity exec --cleanenv \
3   -B ~/intel/oneapi/vtune/latest/:/vtune \
4   -B ${SLURM_TMPDIR}:/data \
5   -B ${PROJECT_DIR}:${PROJECT_DIR} \
6   ${SIF_IMG} \
7   /vtune/bin64/vtune \
8   -collect hpc-performance \
9   -knob enable-stack-collection=true \
10  -knob analyze-openmp=true \
11  -result-dir ${PROFILING_DIR} \
12  <script.sh>

```

Listing 1: Profiling a pipeline within an Apptainer container, using VTune profiler.

We profiled the pipeline using two threading configurations: single-threaded and 32 threads. The single-threaded approach simplified the analysis and limited the potential I/O overhead on the profiling. The 32-thread approach used all available CPU cores from a computing node of our infrastructure to study the multi-threading performance of the pipeline. This configuration provided a more realistic usage of the pipeline.

Before profiling each pipeline, we transferred the input data from the shared file system to the computing node. After profiling, we transferred back the output to the shared file system. This limited profiling variability is due to I/O contingency.

The data generated by the VTune profiler was written to a shared file system, to simplify post-processing. In principle, this could have increased the profiling overhead. However, there was no impact, since the data generated by the VTune profiler was tiny and was not written on the same file system as data produced by the pipelines.

D. Metrics Definition

VTune provides several metrics to characterize the performance of a pipeline. makespan measures elapsed time from the start to the end of the pipeline. The CPU time refers to the total time spent by the CPU, across all cores, to execute the pipeline.

The memory-bound metrics, in particular, focus on identifying bottlenecks where the CPU cannot proceed due to data unavailability. Specifically, memory-bound metrics count the number of cycles where the CPU is stalled waiting for in-flight memory demand loads to be satisfied. This indicates how efficiently or inefficiently the pipeline utilizes memory resources, highlighting scenarios where memory latency hinders performance.

L1 bound occurs when a demand load stalls CPU cores, even though the required data is already in the L1 cache. Similarly, L2, L3, and DRAM bound conditions occur when a demand load causes the CPU to stall due to a cache miss at a particular cache level, with the data instead residing in L2, L3, or DRAM, respectively. In each of these cases, the CPU is delayed while waiting for the requested data to be fetched from the next level in the memory hierarchy.

A store-bound condition arises when a store operation halts CPU execution, often due to insufficient memory bandwidth or resource conflicts. These metrics help isolate whether the performance bottleneck is due to memory bandwidth limitations or inefficient caching. Supplementary Figure 6 shows the monitoring events and equation to derive the metrics defining the memory bound characterization [17]. We use the convention from [18] for the equations.

The difference between the total memory-bound value and the sum of the other metrics indicates the proportion of CPU idle time caused by waiting for data that is missing from all cache levels, meaning the data is being retrieved from secondary storage, such as a disk.

¹<https://github.com/singularityhub/docker2singularity>

E. Infrastructure

We used the *Slashbin cluster* at Concordia University. The compute nodes are configured with two 16-core Intel(R) Xeon(R) Gold 6130 CPU @ 2.10 GHz, 250 GiB of RAM, 126 GiB of tmpfs, six 447 GiB SSDs with the XFS file system (no RAID enabled), Rocky Linux 8.9 and Linux kernel 4.18.0-477.10.1.el8_lustre.x86_64.

III. RESULTS & DISCUSSION

In this section, we present the aggregated profiling data collected using VTune. First, we present a performance overview of the pipelines, then analyze specific hotspots in the pipelines. Unless specified explicitly, we only present the profile data from using 1-thread since the results from 32-threads are similar. We aggregate the profiling results of each pipeline across all subjects to get an average performance profile. Consistently with [18], we hypothesized that the Pareto principle applied to performance of MRI pre-processing pipelines. We therefore only studied the functions with the largest contribution to CPU time, up to 80% cumulative total runtime of the pipeline. This heuristic allowed us to focus our efforts on the performance critical sections of a pipeline. We report the mean and standard deviation of the execution time for those functions.

A. CPU time distribution across functions was long-tailed

Figure 1 shows that 80% of the total CPU time was spent in less than 1.5% of the function across all pipelines. While consistent with the Pareto principle, the distribution of the functions' CPU time did not follow a Pareto distribution. Using the *powerlaw* Python package [19], we found the data fit a Zipf law with an exponent $\alpha = 1.46$ (Supplementary Figure 7). Therefore, the CPU time of a function was approximately inversely proportional to its rank. Thus, future efforts to optimize this minimal set of functions could bring significant performance improvements.

B. Main Bottleneck: Linear Interpolation

Table I shows that interpolation was a critical part of all pipelines except FreeSurfer recon-all, contributing between 32.20% to 62.70% of the total CPU time. Overall, the number of functions using interpolation was low, with less than 20 in each pipeline. Few interpolation functions dominated CPU time. While each interpolation had low computational cost, the large amount of operations resulted in a significant bottleneck. Therefore, optimizing interpolation would bring substantial benefits to these pipelines.

C. Impact of Memory Bounded Functions

Table II shows that fetching data from disks was the main cause for starving the CPU, contributing an average of 6.60% across pipelines. Next, the L1 bound had the highest cache level contribution (5.58% average) to the memory bound of the pipelines. ANTs pipelines had the highest L1 bound, followed by FreeSurfer recon-all and FSL MCFLIRT. L2 and L3 bound were low (0.88% and 1.17% average) for all pipelines, although higher for FreeSurfer recon-all. The DRAM bound

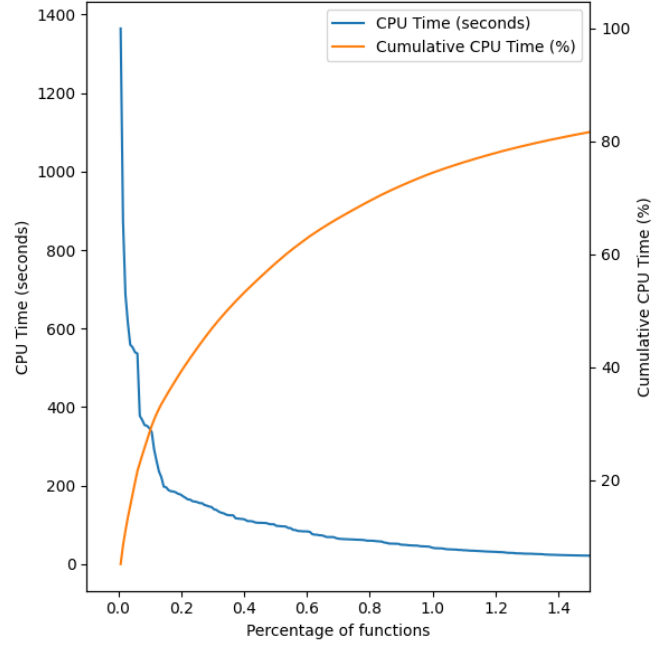


Fig. 1: Distribution of CPU time for the functions. The left y-axis shows the average total CPU Time spent in a function, while the right y-axis shows the cumulative CPU time percentage. The x-axis is the percentage of functions ordered by decreasing CPU time. Data includes functions from all pipelines.

was high for both FSL FLIRT (15.73%) and FreeSurfer recon-all (13.83%), followed by ANTs brainExtraction in double (5.08%) and single (2.48%) precision. Store bound was low for all pipelines. We note an interesting relationship between the low L1 bound and the high DRAM bound of FreeSurfer recon-all and FSL FLIRT, compared to the other pipelines.

Optimizing the data access of the pipeline could reduce the number of data load. This could have a large impact on pipelines performance. Alternatively, the use of reduced precision could reduce the memory footprint, thus the memory bound. To reduce the memory bound impact of fetching data from disks, it could be possible to convert and store the data to a lower precision before pre-processing. In both cases, the impact of reduced precision on the accuracy of the pipelines should be studied.

D. ANTs: Single vs. Double Precision

Figure 2 shows the makespan of ANTs brainExtraction and ANTs registrationSyN with double and single precision. For both pipelines, the makespan was significantly higher in single precision than in double precision. This was unexpected, as the floating-point arithmetic operations are supposed to be faster in single precision than in double precision [20].

ANTs registrationSyN is a three-stage process (Euler transform, affine transform, and SyN registration), where each stage is successively performed at 4 resolution levels with a specified number of maximum iterations. We focused on

Pipeline	# of functions with interpolation	% CPU Time spent in interpolation
ants/brainExtraction	17	38.52
ants/brainExtraction-fp	17	38.37
ants/registrationSyN	7	43.67
ants/registrationSyN-fp	8	47.14
fsl/fast	1	42.97
fsl/mcflirt	3	32.90
fsl/flirt	4	62.07
freesurfer/reconall	10	3.71

TABLE I: Contribution of interpolation to the pipelines’ total CPU time. The percentage is the averaged sum of the CPU time of functions using interpolation. The data includes all functions from all pipelines.

Pipeline	% Memory Bound	% L1 Bound	% L2 Bound	% L3 Bound	% DRAM Bound	% Store Bound	% Disk Bound
ants/brainExtraction	22.61	7.08	0.47	0.81	5.08	0.23	8.94
ants/brainExtraction-fp	20.59	9.11	0.24	0.39	2.48	0.12	8.24
ants/registrationSyN	16.01	6.61	0.79	0.33	0.70	0.44	7.14
ants/registrationSyN-fp	17.97	9.65	0.30	0.08	0.30	0.16	7.48
fsl/fast	9.87	2.87	0.40	0.51	1.61	1.67	2.81
fsl/mcflirt	6.79	3.57	1.96	0.19	0.16	0.10	0.81
fsl/flirt	30.36	1.61	0.42	2.37	15.73	0.59	9.64
freesurfer/reconall	34.07	4.11	2.50	4.69	13.83	1.23	7.72
Average across pipelines	19.78	5.58	0.88	1.17	4.99	0.57	6.60

TABLE II: Impact of data load on stalled CPU cycles. For each metric (Total, L1, L2, L3, DRAM, Store, and Disk Fetch), reported values are summations weighted by function CPU time, averaged over $n = 20$ subjects, and collected in single-threaded mode. They represent the percentage of the total CPU time stalled for the metric.

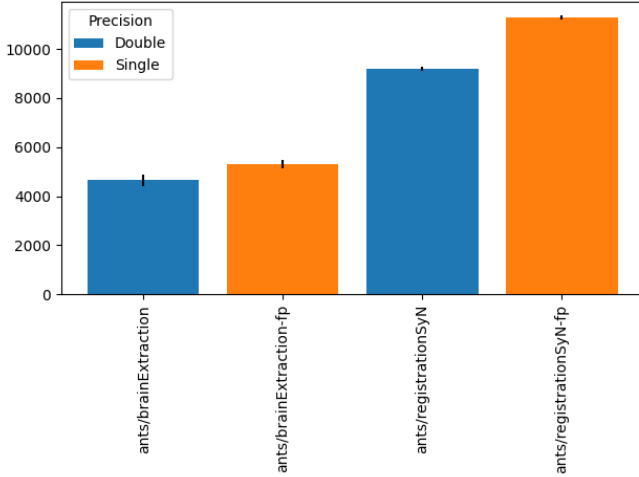


Fig. 2: Comparison of makespan between double (blue) and single (orange) precision for ANTs brainExtraction and ANTs registrationSyN.

the SyN registration stage since it was substantially longer to execute than the other stages. The number of iterations between both versions of ANTs registrationSyN was similar. In fact, for the last two levels, the maximum specified number of iterations was reached across all but one execution. However, the single precision version of ANTs registrationSyN took approximately 20-25% longer per iteration than the double precision version for the last registration stage (Figure 3). Therefore, the slowdown was not due to a slower convergence of the algorithm, but rather to an increased execution time for

each iteration.

After further analysis of the ANTs registrationSyN single-precision pipeline, we found that the use of templates in ITK’s C++ code² forces the output of the interpolation function to be in double precision, with *EvaluateAtContinuousIndex* contributing most to the CPU time. As a result, the pipeline wastes CPU cycles by converting the input data to double-precision in ITK and potentially casting it back to single-precision in ANTs. We think this bug causes the slowdown. We tried re-compiling a version of ITK to fix this issue, but we were unsuccessful because of the size and complexity of the code base. This example shows that the use of reduced precision is not trivial and requires a deep understanding of the code base. Benchmarks should be performed to ensure that the reduced precision does not impact the performance or accuracy of the pipeline. We reported this issue in the ITK GitHub repository³.

E. FreeSurfer: Thread-Synchronization

Figure 4 shows a significant difference in the pipeline profile between single-threaded and multi-threaded executions. In the multi-threaded executions (Figure 4b), the OpenMP multi-threading library was a major bottleneck for the pipeline, accounting for at least 76% of the pipeline runtime. The y-axis scale is multi folds larger than for the single-threaded execution, showing that the multi-threaded execution was significantly slower than the single-threaded execution.

While the makespan for FreeSurfer recon-all decreased with an increase in the number of threads, the benefits were limited

²[itkVectorInterpolateImageFunction.h](https://itk.org/itk/itkVectorInterpolateImageFunction.h)

³<https://github.com/InsightSoftwareConsortium/ITK/issues/4593>

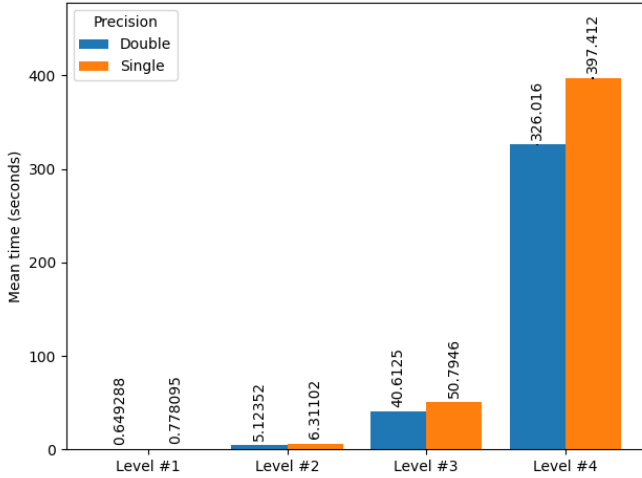


Fig. 3: Average time per iteration for ANTs registrationSyN in double and single precision. Only the SyN Registration stage is shown as the two earlier stages were near zero time. The error bars show the standard deviation across $n = 20$ subjects.

(Figure 5). The parallel efficiency decreased from 66% with two threads down to 5% with 32 threads. While Amdahl’s law limits the maximum parallel efficiency of the pipeline, Figure 4b shows that most of the CPU time is spent in libiomp, which suggests that thread synchronization had a larger impact on parallel efficiency.

OpenMP offers multiple scheduling policies to assign chunks to threads, including *static* scheduling that assigns chunks to threads in round-robin fashion, and *dynamic* which assign chunks to threads as they become available for work. In the codebase, 83 out of 92 tasks use the *static* scheduling policy. This could lead to a load imbalance between the threads, and thus a decrease in parallel efficiency. We speculate that *dynamic* scheduling could improve the parallel efficiency by assigning chunks based on the current load of the threads. Unfortunately, we failed to re-compile FreeSurfer having changed the *static* OpenMP scheduling to *dynamic*. This remains challenging as the codebase is large and complex, and the change in scheduling policy could lead to unexpected bugs. We opened an issue on FreeSurfer GitHub repository to report this problem⁴.

Future work should study the different configuration of OpenMP scheduling in FreeSurfer recon-all to improve the parallel efficiency. We believe that significant performance improvements could be achieved by optimizing the thread synchronization. This would lead to faster runtime time and higher CPU usage ration in HPC allocations.

F. Experiencing using VTune

The VTune profiler provided a rich and extensive amount of data for our analysis, which would have been difficult to retrieve otherwise. Thanks to its low performance overhead,

we could profile the pipeline with minimal impact on the runtime, allowing the use of more subjects to get a more accurate performance profile. The documentation provided by VTune is extensive and well-documented, which helped us to understand the different metrics and events available.

VTune requires a finalization step to query the data and generate a report. We found this step to be both time-consuming and resource intensive. For example, finalizing the results from a single FreeSurfer recon-all execution can require over 2 TB of RAM, while the developers recommend using between 8 GB to 16 GB of RAM to run the pipeline⁵. This significant difference in resource requirement creates a challenge to profile pipeline with long runtime, because of the potential difficulty to get access to computing nodes with enough RAM. One way to mitigate this challenge is to lower the sampling rate during the profiling. However, the sampling rate would have to be significantly reduced for the finalization stage to require a similar amount of RAM (16 GB or less), which would lead to a potential loss of information in the profiling results. Because of these limitations, we could not collect the results of the entire fMRIPrep pipeline, and we only reported results for the sub-pipelines.

IV. CONCLUSION

In this paper, we profiled several MRI pre-processing pipelines used in the popular fMRIPrep tool: ANTs brainExtraction, ANTs registrationSyN, FSL FAST, FSL FLIRT, FSL MCFLIRT, and FreeSurfer recon-all. A few functions were found to contribute significantly to the CPU time, presenting opportunities to optimize these functions and potentially achieve significant speed-up. It was discovered that linear interpolation is the main time bottleneck, with most pipelines being affected by memory bound. We discovered a bug in ITK, which leads to the version of ANTs registration in single precision to use double precision instead. A potential bug in FreeSurfer recon-all was found, which limits the benefit of multi-threading with OpenMP. Last, we discussed the challenge of profiling long-running pipelines with VTune, because of computational resource requirements.

The dataset we chose contains a wide range of age and equal distribution of sex. However, it only contains healthy subjects. It would be interesting to study the impact of image quality and pathologies on performance. Our profiling with VTune did not account for the spatiality (e.g. for loop) or temporality (e.g. start vs. end of convergence) of the functions. This information could provide additional insight for optimization. Future work could extend the depth of the analysis by including this information.

Future optimization efforts could focus on reduced precision techniques, to reduce memory bound and accelerate interpolation computation. We note that the use of reduced precision is not trivial, as seen with the ANTs bug. Therefore, careful attention would be required to find a balance between performance and accuracy. We also suggest for future work

⁴<https://github.com/freesurfer/freesurfer/issues/1199>

⁵<https://surfer.nmr.mgh.harvard.edu/fswiki/SystemRequirements>

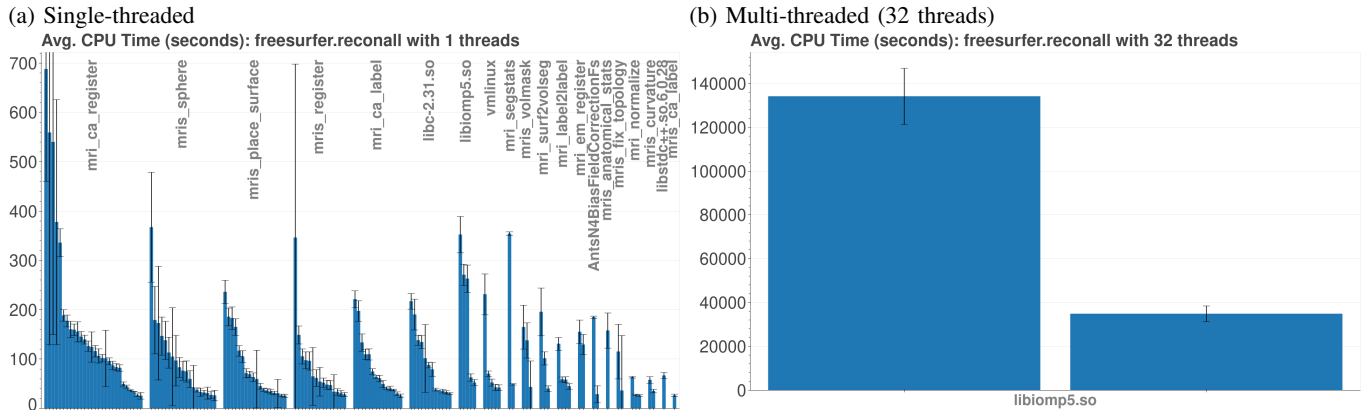


Fig. 4: FreeSurfer recon-all analysis. The y-axis shows the average CPU time spent in each function, with error bars showing the standard deviation across $n=20$ subjects. The x-axis shows the function ordered by decreasing CPU time grouped by module. We only display module names and omitted function names for clarity.

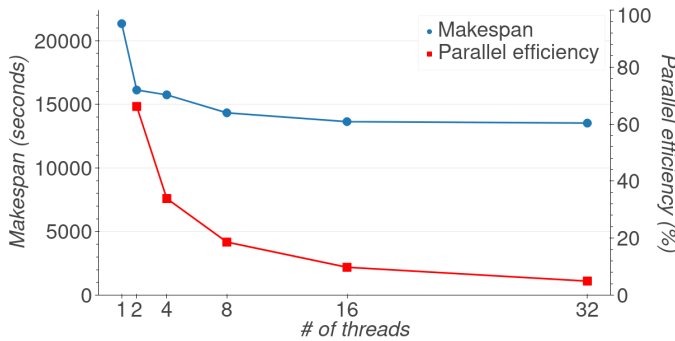


Fig. 5: Makespan and parallel efficiency of FreeSurfer recon-all while varying the number of threads from 1 to 32. The left y-axis shows the makespan in seconds, while the right y-axis shows the parallel efficiency in percent. The log-scaled x-axis shows the number of threads.

to study the different configurations of OpenMP scheduling in FreeSurfer recon-all, to improve parallel efficiency. This would lead to faster executions time and higher CPU usage in HPC allocations.

We hope that this work serves as a reference for future work to optimize MRI pre-processing pipelines.

V. DATA AVAILABILITY

The entire OpenNeuro ds004513 v1.0.2 dataset is freely available to download at:

<https://openneuro.org/datasets/ds004513/versions/1.0.2>.

The container images for our profiling experiments are available on Docker Hub:

- mathdugre/cmake:debug-info
- mathdugre/intel-compilers:debug-info
- mathdugre/afni:debug-info
- mathdugre/ants:debug-info
- mathdugre/fsl:debug-info
- mathdugre/freesurfer:debug-info
- mathdugre/fmripreg:debug-info

Our profiling results from VTune are available at: <https://doi.org/10.5281/zenodo.10987491>

VI. CODE AVAILABILITY

The code to download the data, compile and profile the pipelines, and generate the figures is available at: <https://github.com/mathdugre/mri-bottleneck>

ACKNOWLEDGEMENT

Mathieu Dugré was jointly funded by the Natural Sciences and Engineering Research Council of Canada (NSERC) through the Postgraduate Scholarship-Doctoral (PGS-D) program and the Graduate Doctoral Fellowship Award from Concordia University. This work was partially funded by the Canada Research Chairs program. The computing infrastructure was provided by the Canada Foundation for Innovation.

CONFLICT OF INTERESTS

The authors report no conflict of interests.

REFERENCES

- [1] O. Esteban, C. J. Markiewicz, R. W. Blair, C. A. Moodie, A. I. Isik, A. Erramuzpe, J. D. Kent, M. Goncalves, E. DuPre, M. Snyder, H. Oya, S. S. Ghosh, J. Wright, J. Duriez, R. A. Poldrack, and K. J. Gorgolewski, "fMRIPrep: a robust preprocessing pipeline for functional MRI," *Nature methods*, vol. 16, no. 1, pp. 111–116, Jan. 2019. [Online]. Available: <http://dx.doi.org/10.1038/s41592-018-0235-4>
- [2] Intel, "Intel® VTune™ profiler release notes and new features," <https://www.intel.com/content/www/us/en/developer/articles/release-notes/vtune-profiler-release-notes.html>, accessed: 2024-2-13. [Online]. Available: <https://www.intel.com/content/www/us/en/developer/articles/release-notes/vtune-profiler-release-notes.html>
- [3] B. Avants, N. Tustison, and H. J. Johnson, "Advanced normalization tools (ANTs)," *The insight journal*, Dec. 2020. [Online]. Available: https://psychiatry.ucsd.edu/research/programs-centers/snl/_files/ants2.pdf
- [4] M. Jenkinson, C. F. Beckmann, T. E. J. Behrens, M. W. Woolrich, and S. M. Smith, "FSL," *NeuroImage*, vol. 62, no. 2, pp. 782–790, Aug. 2012. [Online]. Available: <http://dx.doi.org/10.1016/j.neuroimage.2011.09.015>
- [5] B. Fischl, "FreeSurfer," *NeuroImage*, vol. 62, no. 2, pp. 774–781, Aug. 2012. [Online]. Available: <http://dx.doi.org/10.1016/j.neuroimage.2012.01.021>

- [6] R. W. Cox, "AFNI: software for analysis and visualization of functional magnetic resonance neuroimages," *Computers and biomedical research, an international journal*, vol. 29, no. 3, pp. 162–173, Jun. 1996. [Online]. Available: <http://dx.doi.org/10.1006/cbmr.1996.0014>
- [7] N. J. Tustison, B. B. Avants, P. A. Cook, Y. Zheng, A. Egan, P. A. Yushkevich, and J. C. Gee, "N4ITK: improved N3 bias correction," *IEEE transactions on medical imaging*, vol. 29, no. 6, pp. 1310–1320, Jun. 2010. [Online]. Available: <http://dx.doi.org/10.1109/TMI.2010.2046908>
- [8] B. B. Avants, C. L. Epstein, M. Grossman, and J. C. Gee, "Symmetric diffeomorphic image registration with cross-correlation: evaluating automated labeling of elderly and neurodegenerative brain," *Medical image analysis*, vol. 12, no. 1, pp. 26–41, Feb. 2008. [Online]. Available: <http://dx.doi.org/10.1016/j.media.2007.06.004>
- [9] Y. Zhang, M. Brady, and S. Smith, "Segmentation of brain MR images through a hidden markov random field model and the expectation-maximization algorithm," *IEEE transactions on medical imaging*, vol. 20, no. 1, pp. 45–57, Jan. 2001. [Online]. Available: <http://dx.doi.org/10.1109/42.906424>
- [10] A. M. Dale, B. Fischl, and M. I. Sereno, "Cortical surface-based analysis. i. segmentation and surface reconstruction," *NeuroImage*, vol. 9, no. 2, pp. 179–194, Feb. 1999. [Online]. Available: <http://dx.doi.org/10.1006/nimg.1998.0395>
- [11] M. Jenkinson, P. Bannister, M. Brady, and S. Smith, "Improved optimization for the robust and accurate linear registration and motion correction of brain images," *NeuroImage*, vol. 17, no. 2, pp. 825–841, Oct. 2002. [Online]. Available: <https://www.sciencedirect.com/science/article/pii/S1053811902911328>
- [12] M. Jenkinson and S. Smith, "A global optimisation method for robust affine registration of brain images," *Medical image analysis*, vol. 5, no. 2, pp. 143–156, Jun. 2001. [Online]. Available: [http://dx.doi.org/10.1016/S1361-8415\(01\)00036-6](http://dx.doi.org/10.1016/S1361-8415(01)00036-6)
- [13] D. N. Greve and B. Fischl, "Accurate and robust brain image alignment using boundary-based registration," *NeuroImage*, vol. 48, no. 1, pp. 63–72, Oct. 2009. [Online]. Available: <http://dx.doi.org/10.1016/j.neuroimage.2009.06.060>
- [14] T. S. Yoo, M. J. Ackerman, W. E. Lorensen, W. Schroeder, V. Chalana, S. Aylward, D. Metaxas, and R. Whitaker, "Engineering and algorithm design for an image processing api: a technical report on ITK—the insight toolkit," *Studies in health technology and informatics*, vol. 85, pp. 586–592, 2002. [Online]. Available: <https://www.ncbi.nlm.nih.gov/pubmed/15458157>
- [15] G. Castrillon, S. Epp, A. Bose, L. Fraticelli, A. Hechler, R. Belenya, A. Ranft, I. Yakushev, L. Utz, L. Sundar, J. P. Rauschecker, C. Preibisch, K. Kurcys, and V. Riedl, "The energetic costs of the human connectome," 2023. [Online]. Available: <https://openneuro.org/datasets/ds004513/versions/1.0.2>
- [16] G. M. Kurtzer, V. Sochat, and M. W. Bauer, "Singularity: Scientific containers for mobility of compute," *PloS one*, vol. 12, no. 5, p. e0177459, May 2017. [Online]. Available: <http://dx.doi.org/10.1371/journal.pone.0177459>
- [17] Intel, "Intel® 64 and IA-32 architectures software developer's manual," <https://www.intel.com/content/dam/doc/manual/64-ia-32-architectures-optimization-manual.pdf>, 2006. [Online]. Available: <https://www.intel.com/content/dam/doc/manual/64-ia-32-architectures-optimization-manual.pdf>
- [18] "Chapter 6 - introduction to profiling," in *Power and Performance*, J. Kukunas, Ed. Boston: Morgan Kaufmann, Jan. 2015, pp. 105–118. [Online]. Available: <https://www.sciencedirect.com/science/article/pii/B9780128007266000069>
- [19] J. Alstott, E. Bullmore, and D. Plenz, "Powerlaw: a python package for analysis of heavy-tailed distributions," *PloS one*, vol. 9, no. 1, p. e85777, Jan. 2014. [Online]. Available: <http://dx.doi.org/10.1371/journal.pone.0085777>
- [20] N. Wang, J. Choi, D. Brand, C.-Y. Chen, and K. Gopalakrishnan, "Training deep neural networks with 8-bit floating point numbers," Dec. 2018. [Online]. Available: <http://arxiv.org/abs/1812.08011>

SUPPLEMENTARY MATERIALS

$C = CPU_CLK_UNHALTED.THREAD$

$S = CYCLE_ACTIVITY.STALLS_LDM_PENDING$

$O = CYCLE_ACTIVITY.STALLS_L1D_PENDING$

$T = CYCLE_ACTIVITY.STALLS_L2_PENDING$

$W = MEM_L3_WEIGHT$

$H = MEM_LOAD_UOPS_RETIRED.LLC_HIT$

$R = MEM_LOAD_UOPS_MISC_RETIRED.LLC_MISS$

$$M = \frac{W \times R}{H + R}$$

$$N = \frac{H}{H + W \times R}$$

$$\% \text{ Memory Bound} = \frac{S}{C} \times 100 \quad (1)$$

$$\% \text{ L1 Bound} = \frac{S - O}{C} \times 100 \quad (2)$$

$$\% \text{ L2 Bound} = \frac{O - T}{C} \times 100 \quad (3)$$

$$\% \text{ L3 Bound} = \frac{T \times N}{C} \times 100 \quad (4)$$

$$\% \text{ DRAM Bound} = \frac{T \times M}{C} \times 100 \quad (5)$$

Fig. 6: Intel performance monitoring events and derived memory metrics

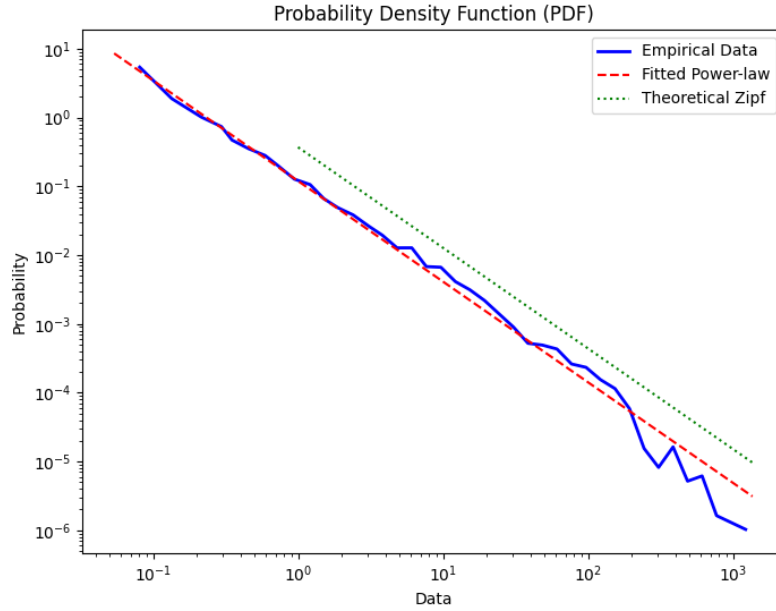


Fig. 7: Distribution of the functions' CPU time compare to a Zipf's law distribution with $\alpha = 1.46$. The y-axis shows the average CPU time for a function. The x-axis shows the percentage of functions ordered by decreasing CPU time. The data includes all functions from all pipelines.

	Module	Function	CPU Time (mean \pm std)	
1	libiomp5.so	``kmp'fork'barrier	134 063.90	\pm 12 810.81
2	libiomp5.so	omp'set'lock	34 815.55	\pm 3599.59

TABLE III: FreeSurfer recon-all (32 threads): Top functions accouting for 80% of the pipeline makespan.